

## TIME TO THE CONVERGENCE OF EVOLUTION IN THE SPACE OF POPULATION STATES

IWONA KAR CZ-DULĘBA\*

\* Institute of Engineering Cybernetics, Wrocław University of Technology  
ul. Janiszewskiego 11/17, 50–362 Wrocław, Poland  
e-mail: kdiwona@ict.pwr.wroc.pl

Phenotypic evolution of two-element populations with proportional selection and normally distributed mutation is considered. Trajectories of the expected location of the population in the space of population states are investigated. The expected location of the population generates a discrete dynamical system. The study of its fixed points, their stability and time to convergence is presented. Fixed points are located in the vicinity of optima and saddles. For large values of the standard deviation of mutation, fixed points become unstable and periodical orbits arise. In this case, fixed points are also moved away from optima. The time to convergence to fixed points depends not only on the mutation rate, but also on the distance of the points from instability. Results show that a population spends most time wandering slowly towards the optimum with mutation as the main evolution factor.

**Keywords:** phenotypic evolution, dynamical system, time to convergence, fixed points

### 1. Introduction

Although easily implemented, evolutionary methods are difficult to analyze theoretically. Usually, a population is considered as a set of individuals evolving in a landscape of a fitness function. However, populations (species), and not individuals, are the main subject of natural evolution. Therefore, it is reasonable to regard the population as a whole. It appears that the idea of considering the population as a point evolving in the space of population states enables the analysis of evolutionary methods and can be fruitful (Vose and Wright, 1994; Galar and Karcz-Dulęba, 1994; Prugel-Bennet, 1997; Vose, 1999). In this paradigm, evolution may be determined by trajectories of an expected population in the space of states. In the general case, the analysis of population dynamics is far from trivial and often some simplifications are required. For example, Vose and Prugel-Bennet examined infinite populations. The opposite place is occupied by very small populations. Our study of a very simple case of phenotypic evolution where a two-element population evolves in one-dimensional search spaces provided very interesting results (Galar and Karcz-Dulęba 1994; Chorążyczewski *et al.*, 2000; Karcz-Dulęba, 2000; 2002; 2004). The expected values of population states generate a discrete dynamical system. For the system its fixed points, their stability and basins of attractions were determined for attributive classes of fitness functions (symmet-

rical, asymmetrical, unimodal, multimodal). The number, location and fixed points' stability depend on the parameters of fitness, and mainly on the evolution parameter — the standard deviation of mutation  $\sigma$ . In this paper, the time to the convergence of the system to fixed points is analyzed. Simulations and analytical considerations will shed light on global and local aspects of the convergence to fixed points. The time to convergence depends on the initial population state. Generally, a low number of generations to convergence characterizes populations initialized at states with a high population quality. A larger  $\sigma$  usually brings about faster convergence, but locations of fixed points move away from optima. Moreover, when the stability of a fixed point is changed, the time to convergence is slowed down.

This paper is organized as follows: In Section 2, models of phenotypic evolution in the space of types and in the space of population states are given. This section provides also the description of two-individual populations in the space of states. The analysis of the population distribution is presented in Section 3. In Section 4, a discrete dynamical system defined by expected states of the population in consecutive iterations is introduced. Its fixed points and their stabilities are presented. Simulation and analytical results of the number of generations to convergence are included in Section 5. Section 6 concludes the paper.

## 2. Model of Phenotypic Evolution in the Space of Population States

In this paper, a simple model of Darwinian evolution (Galar, 1985) is considered. The evolution is phenotypic, asexual and the traits are coded as real numbers. In each generation, a population is composed of  $m$  individuals  $P = \{\mathbf{x}_1, \mathbf{x}_2, \dots, \mathbf{x}_m\}$ . Individuals are described by the  $n$ -element vector of traits (type)  $\mathbf{x}_j = \{x_{j,1}, x_{j,2}, \dots, x_{j,n}\}$ ,  $j = 1, 2, \dots, m$ . To each individual its non-negative performance index (fitness)  $q(\mathbf{x})$  is assigned. Offspring are reproduced asexually in non-overlapping generations. The reproduction rate depends on the individuals' fitness. In a new generation, for each individual a parent is selected according to the proportional selection rule. An offspring inherits its parents' type  $\mathbf{x}$ , modified with the normal distribution  $N(\mathbf{x}, \sigma)$ , where  $\sigma$  denotes the standard deviation of mutation. In the  $(i+1)$ -th generation, the distribution of the new individual's position in  $\mathbb{R}^n$  depends on the positions of individuals in the current ( $i$ -th) generation and is given by

$$\begin{aligned} f_{\mathbf{x}}^{i+1}(\mathbf{x}|P(i)) &= \sum_{k=1}^m \alpha(\mathbf{x}_k^i) g(\mathbf{x}, \mathbf{x}_k^i) \\ &= \sum_{k=1}^m \frac{q(\mathbf{x}_k^i)}{\sum_{j=1}^m q(\mathbf{x}_j^i)} g(\mathbf{x}, \mathbf{x}_k^i), \end{aligned} \quad (1)$$

where  $P(i)$  is the population in the  $i$ -th generation,  $\mathbf{x}_k^i \in \mathbb{R}^n$  stands for the type of the  $k$ -th individual in the  $i$ -th generation,  $\alpha(\mathbf{x}_k^i)$  means the probability of selecting the individual  $\mathbf{x}_k^i$ ,  $q(\mathbf{x}_k^i)$  is the fitness of the individual  $\mathbf{x}_k^i$ , and  $g(\mathbf{x}, \mathbf{x}_k^i)$  signifies the distribution of mutation of the  $k$ -th individual.

The above formulation considers a population in the space of types  $\mathbb{R}^n$  where to each individual a point of the space is assigned. An alternative method is to represent the population as a single point in an appropriately defined *space of population states*  $S$  (Galar and Karcz-Duleba, 1994; Chorażyczewski *et al.*, 2000; Karcz-Duleba, 2000; 2002; 2004). In general, the structure of  $S$  is complicated. The dimensionality of the space of population states is  $m$  times larger than the dimension of the space of types and equal to  $\dim(S) = mn$ . Thus a state of the population in the  $i$ -th generation is described by the vector  $\mathbf{s}^i = (x_{1,1}^i, x_{1,2}^i, \dots, x_{1,n}^i, x_{2,1}^i, x_{2,2}^i, \dots, x_{m,1}^i, \dots, x_{m,n}^i)$ .

The space of population states cannot be identified with  $\mathbb{R}^{mn}$  because the population dynamics do not depend on the ordering of individuals in the population. Therefore, an equivalence relation  $U$  must be defined on  $S$  in order to identify all points corresponding to permutations of individuals within the population. The space

$S$  with  $U$  defined becomes the factor (quotient) space  $S_U = \mathbb{R}^{mn}/U$ .

Further on, two-element populations ( $m = 2$ ) evolving in a one-dimensional search space ( $n = 1$ ) (i.e. (2, 2)-EA) will be analyzed. This simplified case of evolution allows us to keep trace of key mechanisms governing the process. Also, when the whole population is represented as a point  $X = \{x_1, x_2\}$ , it can be visualized easily. In order to define the space of population states  $S_U$ , the following equivalence relation is introduced:

$$\mathbb{R}^2 \rightarrow S_U \subset \mathbb{R}^2 : \quad (x_1^i, x_2^i) \rightarrow \begin{cases} (x_1^i, x_2^i) & \text{for } x_1^i \geq x_2^i, \\ (x_2^i, x_1^i) & \text{for } x_1^i < x_2^i. \end{cases} \quad (2)$$

The mapping identifies the factor space  $S_U$  with the right half-plane bounded by the line  $X_1 = X_2$ , called the *identity axis* (Fig. 1(a)).

In the space of population states the fitness must represent the quality of the entire population, rather than each individual alone. Thus, the fitness function is defined as the average fitness of all individuals from the population ( $\bar{q} = (q(x_1) + q(x_2))/2$ ). In this paper, a bell-shaped Gaussian function with a slope  $a$ ,

$$q(x) = \exp(-ax^2), \quad (3)$$

will serve as an example of the unimodal fitness function. Bimodal fitness functions are represented by the sum of two Gaussian functions with the same slope  $a$  and different heights,

$$q(x) = \exp(-ax^2) + h \exp(-a(x-1)^2). \quad (4)$$

The analysis of evolution in the space  $S_U$  becomes more convenient after the rotation of the  $X_1X_2$  coordinate frame with the angle  $\phi = \pi/4$ . The new coordinate frame, called  $WZ$ , is defined by the transformations  $w^i = (x_1^i - x_2^i)/\sqrt{2}$  and  $z^i = (x_1^i + x_2^i)/\sqrt{2}$ . The factor space  $S_U$  is transformed to the right half-plane ( $w \geq 0$ ) bounded by the  $Z$ -axis (Fig. 1(b)). The population state  $\mathbf{s}^i = (x_1^i, x_2^i)$  is mapped into the state  $\mathbf{s}^i = (w^i, z^i)$ . The new coordinate  $w$  describes the distance of the population state from the identity axis and it may be considered as a measure of the population's diversity. The coordinate  $z$  locates a state along the identity axis.

A few paths of evolution in the space of population states for the unimodal fitness function (3) are depicted in Fig. 1 (in this and further figures, dotted lines correspond to contour lines of the surface of the populations' average fitness  $\bar{q}$ ). Figure 1(a) shows the evolution in the coordinate frames  $X_1X_2$  and Fig. 1(b) illustrates the evolution in the rotated frames  $WZ$ . A population very quickly occupies states near the identity axis, and this indicates its

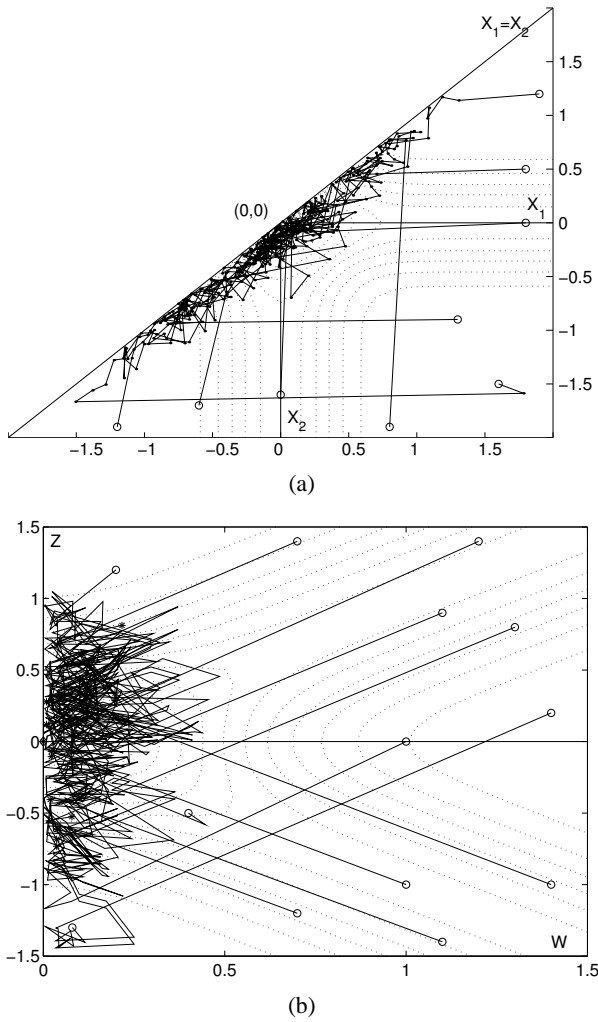


Fig. 1. Evolution of a two-element population in the landscape of the Gaussian unimodal fitness function (3) ( $a = 5$ ). 50 generations are presented for every initial state (marked by an open circle) and  $\sigma = 0.1$ : (a) the coordinate frames  $X_1 X_2$ , (b) the coordinate frames  $W Z$ .

unification. Mainly, the selection mechanism is responsible for the unification of the population. Then the almost homogeneous population slowly approaches the optimum of the fitness function. In the vicinity of the optimum, the population may stay for many iterations, wandering around with steps depending on the standard deviation of mutation  $\sigma$ . This phase of evolution can be called the quasi-equilibrium. Two stages of the process are clearly visible in both the pictures.

### 3. Analysis of Population Distribution

Distributions (1) are the same for each individual and independent of one another. Thus, the joint distribution of the whole population is the product of  $m$  distribu-

tions (1). Since the population state is described in the quotient space, the distribution of the population state in  $S_U$  is given by

$$\begin{aligned} \tilde{f}_{S_U}^{i+1}(\mathbf{s}|\mathbf{s}^i) &= m! \prod_{j=1}^m f_x^{i+1}(\mathbf{x}_j|\mathbf{s}^i) \\ &= m! \prod_{j=1}^m \sum_{k=1}^m \alpha(\mathbf{x}_k^i) g(\mathbf{x}_j, \mathbf{x}_k^i). \end{aligned} \quad (5)$$

Considering a two-element population, the distribution (5) takes the form

$$\tilde{f}_{S_U}^{i+1}(x_1, x_2|\mathbf{s}^i) = 2f_x^{i+1}(x_1|\mathbf{s}^i)f_x^{i+1}(x_2|\mathbf{s}^i). \quad (6)$$

Using the distribution function (6) transformed to new coordinates  $w$  and  $z$ , the expected values of the population state  $\mathbf{s}^i = (w^i, z^i)$  in the next generation can be calculated analytically, see Appendix. The expected values of coordinates  $w$  and  $z$ ,  $E_{i+1}[w|\mathbf{s}^i]$  and  $E_{i+1}[z|\mathbf{s}^i]$ , in the  $(i+1)$ -th generation are respectively equal to

$$\begin{aligned} E_{i+1}[w|\mathbf{s}^i] &= \sqrt{\frac{2}{\pi}}\sigma + \left(1 - \Psi^i\right) \\ &\quad \sigma \left( \phi_0\left(\frac{w^i}{\sigma}\right) + \frac{w^i}{\sigma} \Phi_0\left(\frac{w^i}{\sigma}\right) \right), \end{aligned} \quad (7)$$

$$E_{i+1}[z|\mathbf{s}^i] = z^i + \Psi^i w^i, \quad (8)$$

where

$$\Psi(w, z) = \frac{q((w+z)/\sqrt{2}) - q((z-w)/\sqrt{2})}{q((w+z)/\sqrt{2}) + q((z-w)/\sqrt{2})},$$

$$\Psi^i = \Psi(w^i, z^i),$$

$$\phi_0(\xi) = \frac{1}{\sqrt{2\pi}} \left( \exp\left(-\frac{\xi^2}{2}\right) - 1 \right),$$

$$\Phi_0(\xi) = \frac{1}{\sqrt{2\pi}} \int_0^\xi \exp\left(-\frac{t^2}{2}\right) dt.$$

The expected value (7) is composed of two parts: one depends only on the standard deviation of mutation  $\sigma$  while the other depends also on the current value of  $w$  and on the fitness function (influencing the coefficient  $\Psi$ ). The value of (7) can be lower bounded:  $E_{i+1}[w|\mathbf{s}^i] \geq \sqrt{2/\pi}\sigma$ , since  $q(x)$  is non-negative,  $\phi_0(x) + x\Phi_0(x) \geq 0$ ,  $\Psi \in [-1, 1]$ . While the differences in the fitness values of individuals are significant,  $(1 - \Psi^2) \rightarrow 0$ , we have  $E_{i+1}[w|\mathbf{s}^i] \rightarrow \sqrt{2/\pi}\sigma$ . When the value of the  $w$  coordinate is small, the second component of (7) influences the expected value substantially. The expected value of the  $z$  coordinate (8) depends on the current state of the population and on the sign and the value of the coefficient  $\Psi$  (the fitness of individuals).

The trajectories of the expected values of the population states in the landscape of the unimodal fitness function are presented in Fig. 2. The trajectories reveal a qualitatively similar behaviour to the trajectories of evolution (cf. Fig. 1). Populations initialized at states far from the identity axis very quickly approach the vicinity of the axis, at a distance of about  $\sqrt{2/\pi}\sigma$ . Then, the process of approaching the optimum slows down until it holds up at the equilibrium state. The behaviour of the trajectories could be explained intuitively looking at a population initially consisting of individuals of quite different fitness values. It is very likely that a more fitted individual will be chosen as a parent of both the members of the new population. In this case, the expected distance between offspring depends on the mutation only and it is determined by  $\sigma$ . In a population consisting of individuals of almost equal fitness values, changes in the states will be minor and the movement of the population slows down.

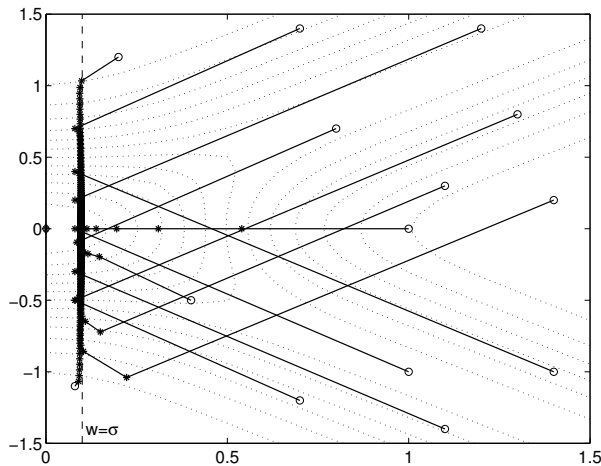


Fig. 2. Trajectories of the expected values of the population states for the unimodal fitness function (3) ( $\sigma=0.1$ ,  $a=5$ ). Asterisks indicate states in consecutive generations.

### 4. Discrete Dynamical System

It is reasonable (as a first approximation of the population behaviour) to assume that the expected value of the population state is just a real point where the population in the next iteration appears. Taking advantage of this interpretation, the expected values of the population state (7) and (8) generate the discrete dynamical system in the space  $S_U$  described by the following equations:

$$\begin{cases} w^{i+1} = E_{i+1} [w|\mathbf{s}^i], \\ z^{i+1} = E_{i+1} [z|\mathbf{s}^i]. \end{cases} \quad (9)$$

Equation (9) defines two scalar mappings

$$(w, z) \rightarrow F(w, z) = \begin{cases} F_1(w, z), \\ F_2(w, z). \end{cases} \quad (10)$$

In the sequel, the analysis of the asymptotic behaviour of the dynamical system (9) is presented.

#### 4.1. Fixed Points of the System

The coordinates of the fixed points of the dynamical system (9) are obtained from the well-known equations  $w = F_1(w, z)$  and  $z = F_2(w, z)$ . The equilibrium states  $\omega = (w^s, z^s)$  are characterized by the conditions

$$w^s \simeq 0.97\sigma, \quad (11)$$

$$\Psi(w^s, z^s) = 0. \quad (12)$$

The  $w$ -coordinate of fixed points (11) depends only on the standard deviation of mutation  $\sigma$ . Since  $w$  indicates the diversity of the population, in the equilibrium state the types of individuals differ about  $\sigma$ . Thus the population is not represented by a single optimal type, as might be expected in the equilibrium state. The  $z$ -coordinate of fixed points depends on a fitness function and it satisfies the equality

$$q\left(\frac{z^s + w^s}{\sqrt{2}}\right) = q\left(\frac{z^s - w^s}{\sqrt{2}}\right). \quad (13)$$

Solutions of (13) are obtained as the points of intersection of two fitness functions  $q_1 = q((z^s + w^s)/\sqrt{2})$  and  $q_2 = q((z^s - w^s)/\sqrt{2})$ . The number of the intersection points depends on the number of the optima of the fitness function and on the standard deviation of mutation. When the value of  $\sigma$  increases, the number of fixed points may decrease as functions  $q_1$  and  $q_2$  are spread apart.

Due to difficulties in obtaining closed-form formulae for the positions of fixed points and other interesting numerical characteristics of evolution for any quality function, one must draw conclusions mainly relying on simulations. A comprehensive description of our previous conclusions (Karcz-Duleba, 2000; 2002) is presented below.

For unimodal fitness functions, the dynamical system (9) has at most one fixed point. When fitness functions are symmetrical, with the optimum placed at zero, the fixed point  $\omega = (0.97\sigma, 0)$  is not placed at the optimum. The smaller  $\sigma$ , the more precise localization of the optimum by the fixed point, but the process of the optimum localization is lengthened. The asymmetry in unimodal fitness functions influences the value of the  $z$ -coordinate of the fixed point leaving its  $w$ -coordinate unchanged. In the case of bimodal fitness functions, the dynamical system (9) has one or three fixed points

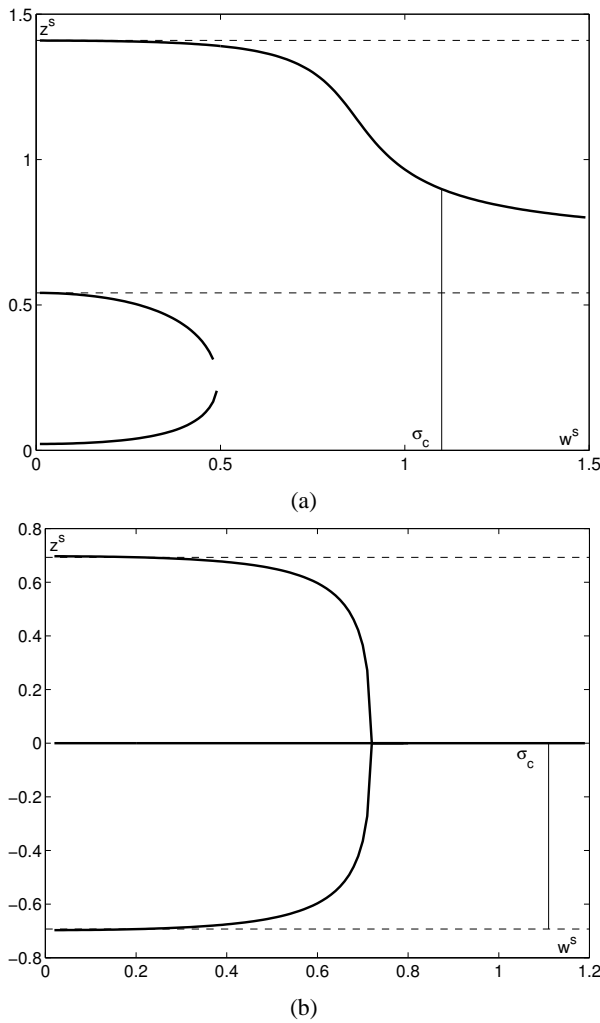


Fig. 3. Location of fixed points as the function of  $w^s$  ( $\sigma$ ), obtained as solutions to (13). Bimodal fitness functions (4) ( $a = 5$ ): (a) asymmetrical ( $h = 2$ ); (b) symmetrical, with the symmetry axis located at zero ( $h = 1$ ).

(Fig. 3(a)), depending on the value of the standard deviation of mutation. For small values of  $\sigma$ , two fixed points are located near optima and one near a saddle. When the standard deviation of mutation is increased, two fixed points disappear and only one fixed point, placed near the global optimum, remains. The symmetry in the fitness function causes symmetry in the localization of the fixed points of two optima and the placement of the third point on the symmetry axis (Fig. 3(b)).

In general, for a fitness function with  $k$  optima, the number of fixed points can vary from 1 to  $2k + 1$ . They are situated near the optima and saddles of a fitness function. For symmetrical fitness functions, one of the points is always located on the symmetry axis while the others are symmetrically paired.

## 4.2. Stability of Fixed Points

To characterize the behaviour of the population in the vicinity of the equilibrium states of the dynamical system, the matrix of its linear approximation must be calculated (Karcz-Dułęba, 2002; 2004):

$$\begin{aligned} & \begin{bmatrix} \frac{\partial F_1(w, z)}{\partial w} & \frac{\partial F_1(w, z)}{\partial z} \\ \frac{\partial F_2(w, z)}{\partial w} & \frac{\partial F_2(w, z)}{\partial z} \end{bmatrix}_{w=w^s, z=z^s} \\ &= \begin{bmatrix} \Phi_0(w) & 0 \\ w \frac{\partial \Psi(w, z)}{\partial w} & w \frac{\partial \Psi(w, z)}{\partial z} + 1 \end{bmatrix}_{w=w^s, z=z^s}. \end{aligned} \quad (14)$$

The linear approximation matrix for the dynamical system (9) is diagonal and its eigenvalues are equal to

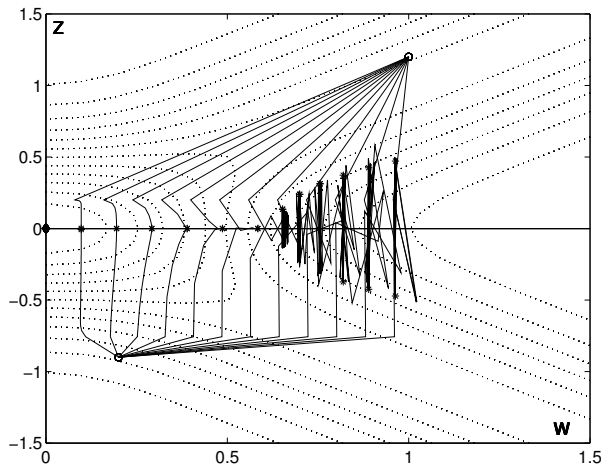
$$\lambda_1 = \Phi_0(w^s), \quad \lambda_2 = w^s \frac{\partial \Psi(w, z)}{\partial z} + 1. \quad (15)$$

Since  $|\lambda_1| < 1$ , the fixed point stability depends on the second eigenvalue only and, consequently, on fitness. The fixed point  $\omega = (w^s, z^s)$  is stable if the inequality

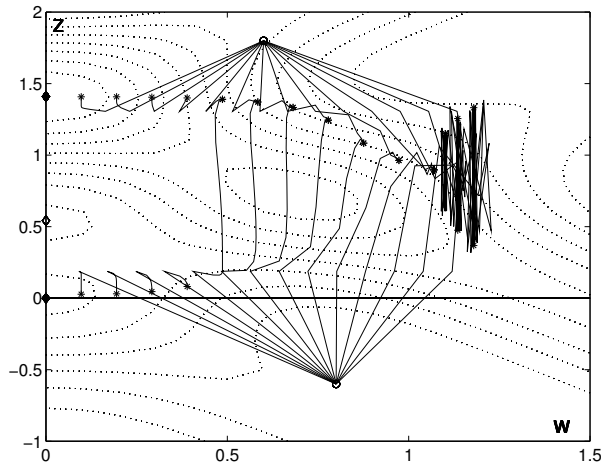
$$-2 \leq w^s \frac{\partial \Psi(w, z)}{\partial z} \leq 0 \quad (16)$$

is satisfied at this point. The fixed point stability depends both on the parameter of the evolutionary process (the standard deviation of mutation) and on the parameters of fitness. It can be proved that saddle fixed points are unstable. Because a fitness function impacts stability, its analysis is provided for specific types of fitness (Fig. 4).

For the unique fixed point  $\omega = (0.97\sigma, 0)$  of the symmetric unimodal Gaussian fitness (3), the condition (16) takes the form  $-2 < -aw^{s^2} < 0$ . The right-hand side of the inequality always holds. Assuming that the parameter  $a$  is given, the fixed point is stable for small values of the standard deviation of mutation  $\sigma$ . For the value  $\sigma_c \simeq \sqrt{2/a}$ , the fixed point loses its stability and a period-doubling (pitchfork) bifurcation appears. For increased  $\sigma$ , stable orbits of period 2 were observed (Fig. 3(a)). For the bimodal fitness (4), fixed points close to optima are stable when  $\sigma$  is relatively small. The fixed point near the global optimum which remains for large  $\sigma$  becomes unstable when  $\sigma$  attains values larger than the distance between the optima. In those circumstances, the fixed point gives rise to a stable orbit of period 2. Simulations performed for even larger values of the standard deviation of mutation  $\sigma$  do not exhibit any other periodic orbits. However, differences in fitness values for large  $\sigma$  are so insignificant that round-off errors could be of concern.

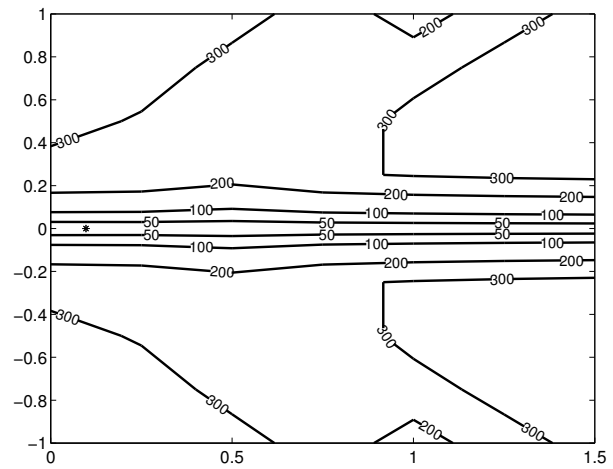


(a)

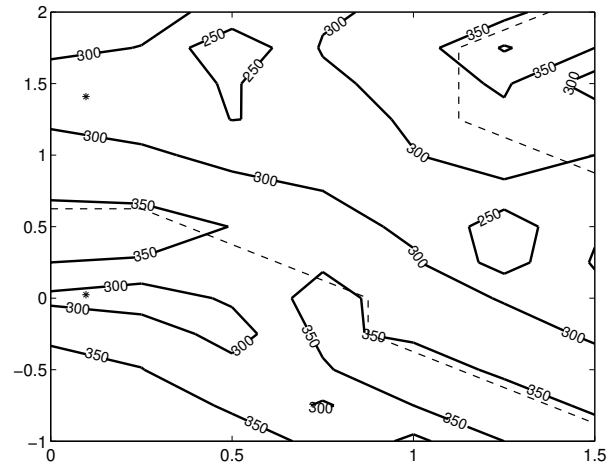


(b)

Fig. 4. Trajectories of the dynamical system (9) for different values of  $\sigma$ . Stable fixed points and periodical orbits are observed. The initial states are denoted by open circles and the fixed points by asterisks: (a) unimodal fitness function (3) ( $a = 5$ ),  $\sigma \in [0.1, 1.2]$ ; (b) bimodal fitness function (4) ( $a = 5$ ,  $h = 2$ )  $\sigma \in [0.1, 1.4]$ , the step for  $\sigma$  equal to 0.1.



(a)



(b)

Fig. 5. Number of generations to convergence for  $\sigma = 0.1$ . Fixed points are marked by asterisks. Dotted lines separate the basins of attractions of both optima. Initial states are located on the grid  $w \in [0, 1.5]$ ,  $z \in [-1, 1]$  and  $z \in [-1.5, 1.5]$ , respectively, for (a) and (b) with step 0.25: (a) unimodal fitness (3) ( $a = 5$ ); (b) bimodal fitness (4) ( $a = 5$ ,  $h = 2$ ).

### 5. Time to Convergence

The number of generations needed to reach the optimum is an important feature of optimization methods. The time to the convergence to a fixed point can be also analyzed in the case of the dynamical system (9). We start with simulation results. In Fig. 5, the numbers of generations to convergence to fixed points for unimodal and bimodal fitness functions are presented. The diagram shows the number of generation needed to stabilize (i.e., the absolute difference between coordinates  $w$  and  $z$  of two consecutive points drops below the prescribed value of  $\epsilon = 10^{-8}$ ) for initial states located on a grid covering the visualized area. The value of  $\epsilon$  was determined empirically to preserve a

satisfactory accuracy of finding the fixed point with a reasonable amount of computations. Increasing precision (by taking smaller values of  $\epsilon$ ) does not influence the shape of the diagram but increases the number of generations needed to find the fixed point. For unimodal fitness, the smallest numbers of generations to reach the stable state are observed for populations initially located on and along the  $w$  axis. A few more generations were needed for initial states with one almost optimal individual in the population (two ridges in the average surface of the fitness). The largest number of iterations to stabilize the population was required for populations initialized at states with small values of the average fitness. It appears (Fig. 5(b)) that for the bimodal fitness function, initial states from

which evolution is relatively fast coincide with the basin of attraction of the global optimum (Karcz-Dulęba, 2004).

The earlier analysis of the dynamical system (9) revealed that the evolution distinguished states located on the line parallel to the  $Z$  axis and placed at a distance of  $w = \sqrt{2/\pi}\sigma$  from the axis. Therefore, it is interesting to answer the question how many generations are required to bring the population to the vicinity of the line for various quality functions. (For simplicity, it was checked how fast the coordinate  $w$  drops below the value of  $\sigma$ . Further on, the line  $w = \sigma$  is referred to as the  $\sigma$ -line.) In Fig. 6 attraction abilities of the  $\sigma$ -line are demonstrated for uni- and bimodal fitness functions. The number of generations needed to get to the  $\sigma$ -line is much smaller than the num-

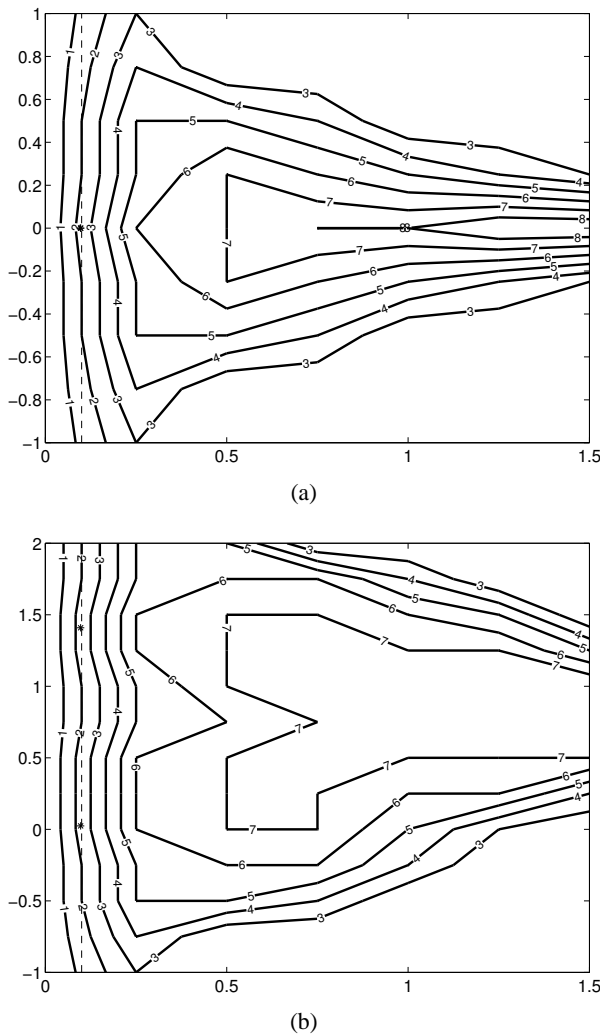


Fig. 6. Number of generations to reach the  $\sigma$ -line for  $\sigma = 0.1$ . Fixed points are marked by asterisks and the  $\sigma$ -line is depicted by the dotted line. As for the initial states, cf. Fig. 5. Results: (a) unimodal fitness function (3), ( $a = 5$ ); (b) bimodal fitness function (4), ( $a = 5, h = 2$ ).

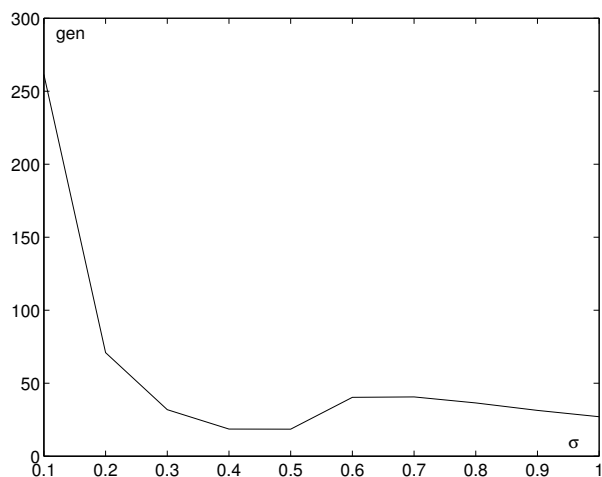
ber needed to reach fixed points. On the average, only a few generations are necessary to move the population to the neighbourhood of the  $\sigma$ -line for the tested fitness functions. This effect does not depend on the value of  $\sigma$  and it corresponds to jumps of trajectories, observed in the simulation of evolution and in the dynamical system analysis (see Figs. 1 and 2). For most of the time (measured in generations), the population wanders in the vicinity of the  $\sigma$ -line, where the differences in the types of individuals are about  $\sigma$ . Since  $\Psi \in [-1, 1]$ , in one iteration the population cannot move along the  $z$ -axis by more than  $\sigma$ , cf. (8) and (9).

The average time to the convergence to the fixed point decreases considerably when  $\sigma$  increases, for both uni- and bimodal fitness functions (Fig. 7). For large  $\sigma$ , the population needs fewer than a hundred generations to reach a stable state. However, it is not good advice to set the parameter  $\sigma$  to a large value. Although the time of evolution is short, the distance of the fixed point to the optimum is significant. The sharp peak in Fig. 7(b) occurs near the bifurcation point and it is a consequence of stability changes (convergence to the orbit, rather than to the fixed points). The increase in the number of generations to converge near the bifurcation point is also observed for the unimodal function, but the increment is not so crucial.

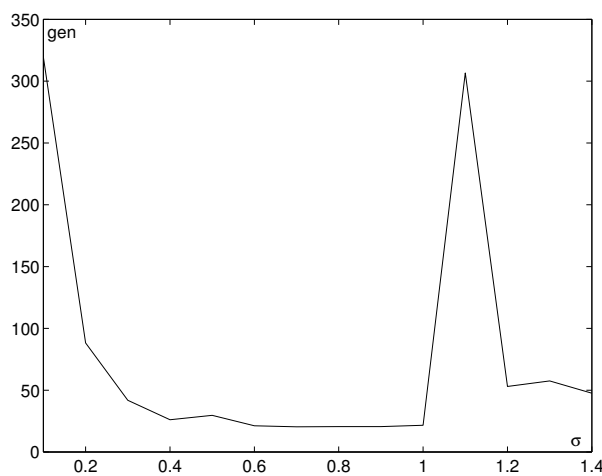
Till now, the (global) time to the convergence to the global optimum or to the attraction  $\sigma$ -line have been analyzed. There also exists a local view on convergence time to fixed points. The analysis of the absolute values of the eigenvalues given by (15) allows us to trace the time in a close neighbourhood of fixed points. Obviously, assuming the stability of a fixed point, time to convergence is determined by the eigenvalue which attains a larger absolute value than the other eigenvalue. Let us have a closer look at the case of population evolution in a close vicinity of the fixed point with the unimodal Gaussian fitness (3). For very small values of  $\sigma$ ,  $|\lambda_1| \simeq 0$  while  $|\lambda_2| \rightarrow 1$  and convergence to the stable point is very slow. When  $\sigma$  increases, so does  $|\lambda_1|$ , while  $|\lambda_2|$  decreases. Two interesting values of  $\sigma$  can be distinguished, namely, those characterized by the condition

$$|\lambda_1(\sigma)| = |\lambda_2(\sigma)|, \quad (17)$$

when the time to convergence to the fixed point is not slowed down by any eigenvalue. In Fig. 8, the absolute values of the eigenvalues for the unimodal fitness function (3) are presented. Comparing the shapes of Fig. 8 and Fig. 7(a) ( $\sigma \in [0.2, 0.6]$ ) one can notice that the local view on convergence corresponds to the global view. It allows us to claim (at least for the case of the fitness considered) that the motion along the  $\sigma$ -line reveals the same dynamics as the behaviour around the fixed point.



(a)



(b)

Fig. 7. Average time to reach the fixed point or orbit, as a function of  $\sigma$ . The number of generations is averaged from 90 trajectories started from states located on the grid (see Fig. 5). Results: (a) unimodal fitness function (3), ( $a = 5$ ); (b) bimodal fitness function (4), ( $a = 5, h = 2$ ).

## 6. Conclusions

In this paper phenotypic evolution of two-element populations evolving in a one-dimensional search space was considered. The discrete dynamical system derived from the evolution of the expected location of the population in the space of population states was analyzed. The time to the convergence to fixed points of the system was of particular interest. The evolution process appeared to be a two-speed process. Its first phase, a fast approach to states located at a distance of about  $\sigma$  from the  $Z$ -axis is followed by slow convergence to the fixed point afterwards. The jump to the  $\sigma$ -line indicates the unification of the population. When the population becomes almost

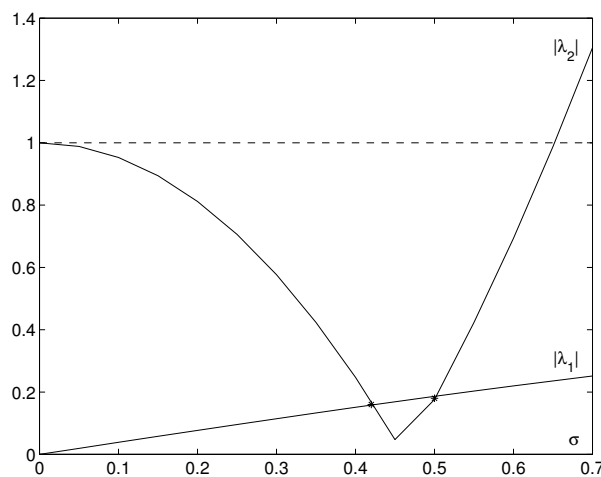


Fig. 8. Absolute values of the eigenvalues of the dynamical system (9) for the unimodal fitness (3) with  $a = 5$ .

homogeneous, individuals differ by about  $\sigma$ . With such small differences in the types of individuals, the selection pressure is low and the population movement slows down. Simulations and the analysis of the eigenvalues of the dynamical system allow us to formulate some hints about how to set the mutation parameter  $\sigma$ . Too small values substantially slow down the convergence but the optimum is reached more precisely than in the case of large values of  $\sigma$ . In the latter case, to some extent, the number of generations to convergence is small but fixed points are placed at some distance from optima. Moreover, when  $\sigma$  is large enough, fixed points lose their stability and once again the time to convergence is low. For researchers implementing evolutionary search methods, it is advised to vary the mutation rate depending on the phase of the optimization process.

## References

Chorażyczewski A., Galar R. and Karcz-Duleba I. (2000): *Considering phenotypic evolution in the space of population states.* — Proc. 5th Conf. Neural Networks and Soft Computing, Zakopane, Poland, pp. 615–620.

Galar R. (1985): *Handicapped individua in evolutionary processes.* — Biol. Cybern., Vol. 51, No. 1, pp. 1–9.

Galar R. and Karcz-Duleba I. (1994): *The evolution of two: An example of space of states approach.* — Proc. 3rd Ann. Conf. Evolutionary Programming, San Diego, CA, pp. 261–268.

Karcz-Duleba I. (2000): *Dynamics of evolution of population of two in the space of population states. The case of symmetrical fitness functions.* — Proc. 4th Nat. Conf. Evol. Algorithms and Global Optimization, Łądek Zdrój, Poland, pp. 115–122 (in Polish).



- Karcz-Duleba I. (2002): *Evolution of two-element population in the space of population states: Equilibrium states for asymmetrical fitness functions*, In: *Evolutionary Algorithms and Global Optimization* (J. Arabas, Ed.). — Warsaw: Warsaw University of Technology Press, pp. 35–46.
- Karcz-Duleba I. (2004): *Asymptotic behavior of discrete dynamical system generated by simple evolutionary process*. — *Int. J. Appl. Math. Comp. Sci.*, Vol. 14, No. 1, PP. 79–90.
- Prugel-Bennett A. (1997): *Modeling evolving populations*. — *J. Theor. Biol.*, Vol. 185, No. 1, pp. 81–95.
- Vose M.D. and Wright A. (1994): *Simple Genetic Algorithms with Linear Fitness*. — *Evolut. Comput.*, Vol. 2, No. 4, pp. 347–368.
- Vose M.D. (1999): *The Simple Genetic Algorithm. Foundations and Theory*. — Cambridge, MA: MIT Press.

## Appendix

The distribution of the population state in the quotient space  $S_U$  (5) for two-element populations is given by

$$\begin{aligned} \tilde{f}_{S_U}^{i+1}(x_1, x_2 | \mathbf{s}^i) &= 2f_X^{i+1}(x_1 | \mathbf{s}^i) f_X^{i+1}(x_2 | \mathbf{s}^i) \quad (18) \\ &= 2 [\alpha(x_1^i) g(x_1, x_1^i) + \alpha(x_2^i) g(x_1, x_2^i)] \\ &\quad \times [\alpha(x_1^i) g(x_2, x_1^i) + \alpha(x_2^i) g(x_2, x_2^i)], \end{aligned}$$

where

$$\alpha(x_k^i) = \frac{q(x_k^i)}{q(x_1^i) + q(x_2^i)}$$

and

$$\begin{aligned} g(x_j, x_k^i) &= N(x_k^i, \sigma) \\ &= \frac{1}{\sqrt{2\pi}\sigma} \exp\left(-\frac{(x_j - x_k^i)^2}{2\sigma^2}\right), \quad k = 1, 2. \end{aligned}$$

The coordinate frame  $X_1 X_2$  is rotated by the angle  $\phi = \pi/4$  and transformed to new coordinates  $WZ$ , where  $w = (x_1 - x_2)/\sqrt{2}$  and  $z = (x_1 + x_2)/\sqrt{2}$ . After the rotation, the factor space  $S_U$ , originally identified with the right half-plane bounded by the line  $X_1 = X_2$ , becomes the right half-plane  $w \geq 0$  bounded by the  $Z$  axis.

The expected values of state  $\mathbf{s}^{i+1}$  in coordinates  $WZ$  are calculated as

$$\begin{aligned} E_{i+1}[w | \mathbf{s}^i] &= \int_0^\infty \int_{-\infty}^\infty w \tilde{f}_{S_U}^{i+1}(w, z | \mathbf{s}^i) dz dw, \\ E_{i+1}[z | \mathbf{s}^i] &= \int_0^\infty \int_{-\infty}^\infty z \tilde{f}_{S_U}^{i+1}(w, z | \mathbf{s}^i) dz dw, \quad (19) \end{aligned}$$

using the distribution (18) transformed into the new coordinates. After integration, the expected values take the forms (7) and (8).